NASA/CR—2004-213317

Analysis of the Spread Across Liquid–5 (SAL–5) Experiment Failure to Fill Properly During Flight

Jeffrey S. Allen
National Center for Microgravity Research, Cleveland, Ohio

September 2004

The NASA STI Program Office . . . in Profile

Since its founding, NASA has been dedicated to the advancement of aeronautics and space science. The NASA Scientific and Technical Information (STI) Program Office plays a key part in helping NASA maintain this important role.

The NASA STI Program Office is operated by Langley Research Center, the Lead Center for NASA's scientific and technical information. The NASA STI Program Office provides access to the NASA STI Database, the largest collection of aeronautical and space science STI in the world. The Program Office is also NASA's institutional mechanism for disseminating the results of its research and development activities. These results are published by NASA in the NASA STI Report Series, which includes the following report types:

- TECHNICAL PUBLICATION. Reports of completed research or a major significant phase of research that present the results of NASA programs and include extensive data or theoretical analysis. Includes compilations of significant scientific and technical data and information deemed to be of continuing reference value. NASA's counterpart of peer-reviewed formal professional papers but has less stringent limitations on manuscript length and extent of graphic presentations.

- TECHNICAL MEMORANDUM. Scientific and technical findings that are preliminary or of specialized interest, e.g., quick release reports, working papers, and bibliographies that contain minimal annotation. Does not contain extensive analysis.

- CONTRACTOR REPORT. Scientific and technical findings by NASA-sponsored contractors and grantees.

- CONFERENCE PUBLICATION. Collected papers from scientific and technical conferences, symposia, seminars, or other meetings sponsored or cosponsored by NASA.

- SPECIAL PUBLICATION. Scientific, technical, or historical information from NASA programs, projects, and missions, often concerned with subjects having substantial public interest.

- TECHNICAL TRANSLATION. English-language translations of foreign scientific and technical material pertinent to NASA's mission.

Specialized services that complement the STI Program Office's diverse offerings include creating custom thesauri, building customized databases, organizing and publishing research results . . . even providing videos.

For more information about the NASA STI Program Office, see the following:

- Access the NASA STI Program Home Page at ***http://www.sti.nasa.gov***

- E-mail your question via the Internet to help@sti.nasa.gov

- Fax your question to the NASA Access Help Desk at 301–621–0134

- Telephone the NASA Access Help Desk at 301–621–0390

- Write to:
  NASA Access Help Desk
  NASA Center for AeroSpace Information
  7121 Standard Drive
  Hanover, MD 21076

NASA/CR—2004-213317

Analysis of the Spread Across Liquid–5 (SAL–5) Experiment Failure to Fill Properly During Flight

Jeffrey S. Allen
National Center for Microgravity Research, Cleveland, Ohio

Prepared under Contract NCC3–975

National Aeronautics and
Space Administration

Glenn Research Center

September 2004

Available from

NASA Center for Aerospace Information
7121 Standard Drive
Hanover, MD 21076

National Technical Information Service
5285 Port Royal Road
Springfield, VA 22100

Available electronically at http://gltrs.grc.nasa.gov

Analysis of the Spread Across Liquid–5 (SAL-5) Experiment Failure to Fill Properly during Flight.

Jeffrey S. Allen
National Center for Microgravity Research
Cleveland, Ohio 44135

1 Filling the SAL-5 Fuel Tray - Ideal Conditions

Under ideal flight conditions, the Spread Across Liquids (SAL-5) fuel tray should fill in a sequence of steps each of which is governed by a unique physical mechanism. Initially, the correct volume of liquid is *mechanically* pumped into the fuel tray in a controlled manner. Then, *wicking* in the corners of the fuel tray redistributes the liquid uniformly around the periphery of the fuel tray. As the wicking occurs, the liquid is also *spreading* across the bottom surface of the fuel tray. After the liquid has completely wetted all of the tray surfaces (sides, ends, and bottom), then *capillary pressure* will cause the liquid will flow so as to minimize the surface area. If the correct liquid volume is present in the fuel tray, then the minimum surface area is that of a flat, or level, surface. All of the above events have to occur in order to properly fill the fuel tray.

In addition, the SAL-5 flight experiment required proper filling of the fuel tray in a short period of time; approximately 4 minutes of experiment time with an expected fill time of 2 minutes. There is a time scale associated with each of the fill events described above and the total fill time must be within the experiment constraints. Figure 1 illustrates an idealized filling process; illustrating the beginning and end of each event during the fill process. The mechanical pump time is the time required to pump the proper volume of liquid into the fuel tray. The wicking time is the time required to redistribute the liquid uniformly around the periphery of the fuel tray. Within the wicking time is the corners-wetted-time which is the time required for the liquid to wick around the periphery of the fuel tray (i.e., the time required for the liquid tips in the corners to meet at the end opposite of the fill port.) The spreading time is the time required to completely wet the bottom surface of the fuel tray. Finally, the leveling time is the time required for the liquid to minimize its surface area.

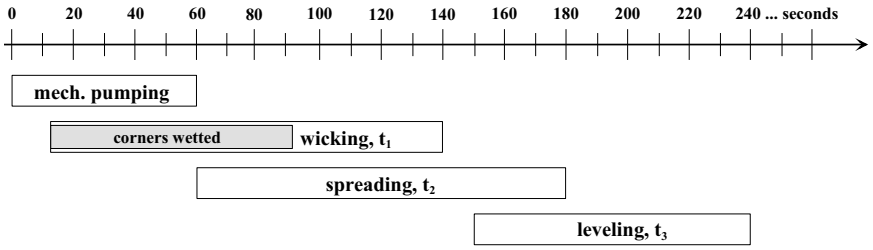

Figure 1. Idealized timeline for filling the SAL-5 fuel tray. These times reflect ideal conditions and not actual flight times. Note that the spreading and leveling times were not considered prior to the SAL-5 flight.

During the SAL-5 flight, the fuel tray did not fill within the allotted time; resulting in failure of the experiment. The failure to fill could be the result of any one (or combination) of the fill events not occurring properly or if the time to complete any of the events was too long.

2 Failure to Fill the SAL-5 Fuel Tray

The SAL-5 flight video clearly shows that liquid did not wick along the one corner of the fuel tray. In addition, as the liquid spread the contact line "pinned" in various locations which indicated contamination of the fuel tray surface. The initial assessment was that the failure to properly fill during flight was because of the inability to wick along one side of the fuel tray.

From the flight video, it is apparent that the wicking did not occur because the liquid did not fill the gap between the glass side wall and fuel tray. This resulted in an exceptionally long contact line and wicking

only on the opposite wall. There could be several reasons for the liquid not filling the gap, but this problem is not necessarily the reason for the tray not filling properly. Questions which must be answered are:

1. Why did the liquid not fill the gap on one side?

   This could be the result of the fuel tray acting as a pinning edge, contamination of the liquid, and/or contamination of the fuel tray surface. The liquid did fill the gap on one side; most likely because of the presence of a small piece of felt inserted into the gap at the fill port and ignitor ends of the fuel tray. The felt was placed into this side in order to facilitate liquid filling the gap after ground-based fill tests failed. Even though the gap on the opposite side did fill during the ground-based tests, the reason felt was not placed into this gap was because the gap was too narrow for the felt to be inserted.

   It is important to note that due to the presence of the gaps, redistribution of the liquid via capillary flow in the corners can not occur unless the gaps are filled with liquid. Thus, another time scale is introduced; that is, the time required for liquid to enter the gap. On the side with the felt pieces, this time is essentially zero. However, on the opposite side (without the felt), the time to fill the gap was greater than the experiment time.

2. Assuming that both gaps had filled with liquid, would the fuel tray have filled properly in the allotted time?

   The answer to this question requires investigating a sequence of events which must occur properly in order to fill the SAL-5 fuel tray.

   - Was the correct volume of liquid pumped into the fuel tray?
   - Was the analysis used to determine the wicking time appropriate?
   - Were the fuel tray conditions used in the wicking analysis correctly modeled?
   - Was the assumption that the wicking of liquid in the corners is the limiting factor appropriate?
   - What are the appropriate time scales for liquid spreading and liquid leveling?
   - Could contamination have significantly affected the timescales for wicking, spreading, and/or leveling?

3 Contamination

The suspicion of contamination arose from observations of the flight video. While filling the fuel tray during flight, the liquid front, or contact line, did not advance smoothly. Instead, at various locations along the fuel tray the contact line would "pin" resulting in a local change in curvature of the liquid surface. In other words, a small dimple would form at the point where the contact line would pin.

Examination under a microscope revealed many scratches in the surface of the fuel tray. In particular, large scratches perpendicular to the glass side wall on the side with the large gap were observed. The scratches were approximately 1 mm long and were located in the regions where excess RTV was removed using a razor blade. Coincidentally, the location of the scratches also appeared to correlate to the locations of contact line pinning.

3.1 Testing for Contamination

Contamination of the fuel tray was tested by placing small drops of n-butanol on the various fuel tray surfaces and examining the spread and shape of the drop. A uniform, wetting drop indicates that there is no contamination. A ragged drop perimeter indicates mixed wetting conditions indicative of heterogeneous contamination. A smooth, non-wetting drop indicates that the surface is uniformly coated with some surface agent. The static contact angle is used as a measure of surface contamination. Baseline tests were conducted on known samples of anodized aluminum in order to determine the contact angle of a non-contaminated

drop. Details of calculating the contact angle from the final drop diameter and the drop volume are given in Appendix B.1.

The initial locations for testing on the fuel tray were taken from the "dimple" points on the flight video. Additional points were chosen based upon observation through the microscope as well as a few random locations. Table 4 in Appendix A lists all of the locations for testing of contamination for the SAL-5 fuel tray and the location of each test point is illustrated in Figure 7.

During these fifty tests, the drops placed on the bottom surface of the fuel tray were not circular or uniform. The SAL-5 fuel tray was found to be a very heterogeneous surface with numerous small patches ($\sim$1 mm in diameter) where the n-butanol did not want to wet; indicating non-uniform contamination. There was no location found on the bottom surface of the fuel tray where this heterogeneity was not found. Figure 2 illustrates the general contamination of the fuel tray surface. The image is of two 10 μliter drops of n-butanol on the flight fuel tray. The drops have ceased to increase in diameter indicating that spreading has stopped. Note the ragged shape of these two drops.

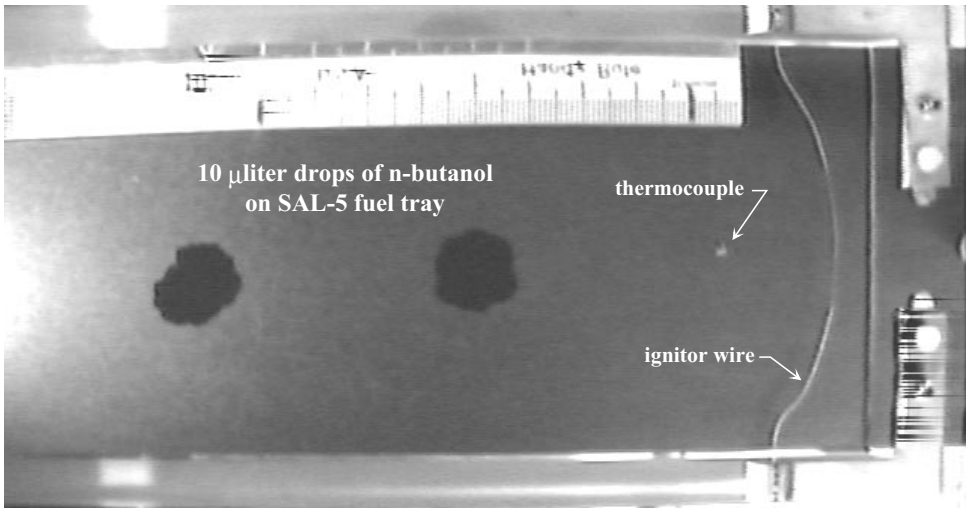

Figure 2. Image from spreading tests conducted on the flight fuel tray. The two drops are both 10 μliters and show a non-uniform contact line indicating a heterogeneous surface. A homogeneous surface would result in uniform, circular drops.

A higher level of contamination was found in a 1–2 mm strip along each of the glass side walls. These non-wetting strips are visible under the right lighting conditions. It was difficult to place n-butanol on these strips because of the degree of non-wettability; in most cases the liquid had to be forced onto these strips by dragging the drop with the syringe needle. The liquid response to this non-wetting strip is illustrated in Figure 3 where a 39 μliter drop is placed near the side wall of the fuel tray. The portion of the drop which covers the contamination strip was forced there using a syringe needle.

The barrier coating (3M FC-723) applied to the top of the glass side walls and to the top of the end plates was found to be intact and robust during the testing. Also, the side of one glass wall was found to have a relatively high contact angle indicating contamination. The side of the other glass wall was not tested. Tests on the ignitor brackets found that n-butanol perfectly wets this material. In general, the fuel tray was found to be heterogeneous patchwork of contamination sites with the exceptions of a thin strip along each glass wall and the side of the glass walls. The contamination on these exceptions was found to be uniform, but resulted in a much higher contact angle than the bottom of the fuel tray. The highest contact angle was found to be on the barrier coating. The scratches near the glass side wall described earlier were within the thin strip of high contamination. In other words, the liquid stopped spreading when it reached the high contamination strip; before encountering the observed scratches. This can be seen in Figure 4 where the liquid drop stopped spreading towards the wall well before reaching the scratches in the edge of the fuel tray.

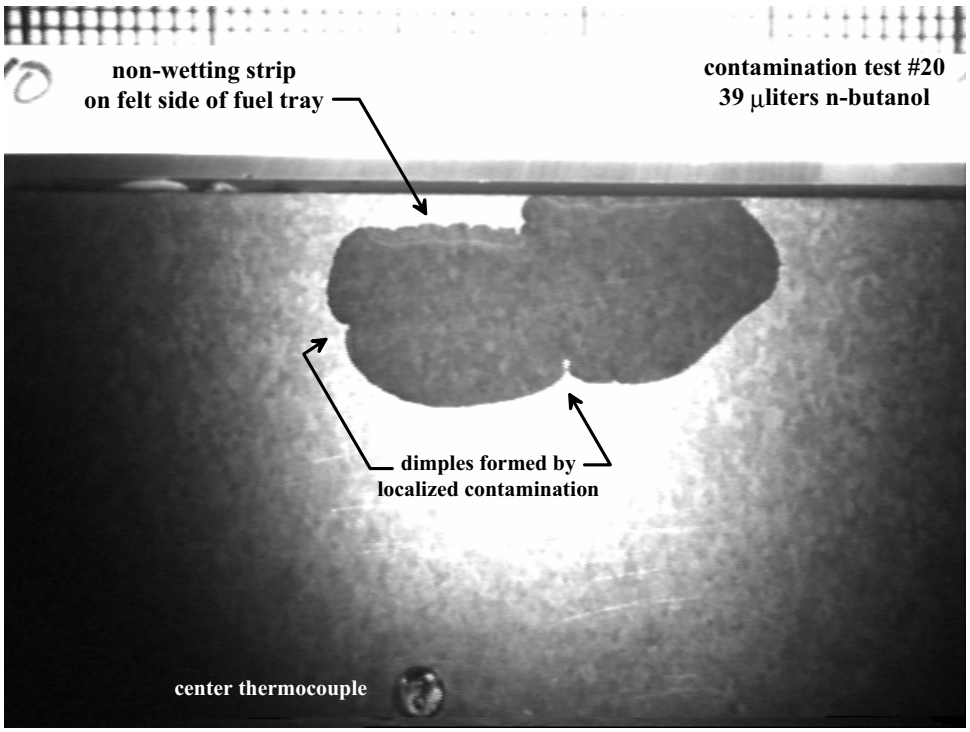

Figure 3. Image from contamination test #20 at 39 μliters. The syringe needle was used to drag a portion of the drop over the non-wetting strip next to the side wall.

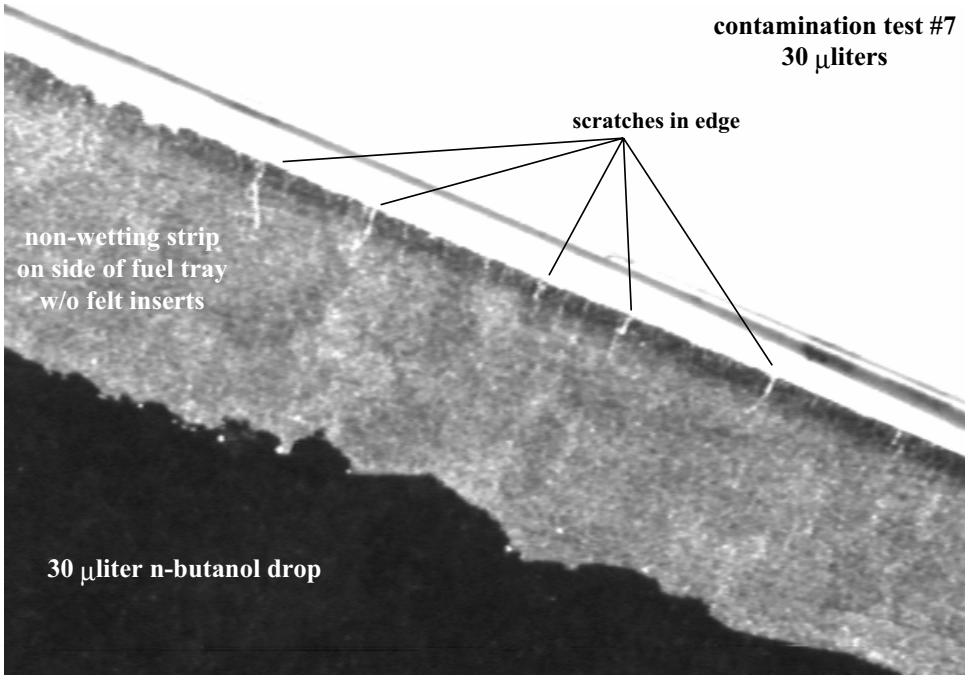

Figure 4. Image from contamination test #7 at 30 μliters. The drop stopped spreading towards the glass side wall after contacting the non-wetting strip. The scratches in the edge of the fuel tray are within the non-wetting strip; hence, the liquid does not encounter the scratches.

3.2 Potential Sources of Contamination

Determining the source of contamination is extremely difficult and it is unlikely that the exact cause can be quantified. However, a list of potential sources of contamination has been developed and studied.

1. Technical grade acetone: used for cleaning fuel tray surfaces. A technical grade of acetone was used to clean the fuel tray surfaces after each normal gravity burn test. Tissues and cotton swabs were used to apply the acetone.

2. Barrier coating: applied to the top of the glass walls in order to inhibit the spread of n-butanol outside of the fuel tray. The barrier coating was reapplied after every ground-based flame test. The barrier coating used for the SAL-5 experiment was Fluorad™ Surface Modifier FC-723 manufactured by 3M Corporation. FC-723 is a flouro-chloro based hydrophobic polymer that deposits a low surface energy film on a substrate. The purpose of applying FC-723 to the glass side walls of the SAL-5 fuel tray was to contain the n-butanol. The hydrophobic film deposited on the glass walls helps to prevent the n-butanol from spilling out of the fuel tray.

3. RTV: used to secure glass side walls to the fuel tray. During the assembly process, the surfaces in the vicinity of the RTV may have been wetted by the RTV solvent. If so, the solvent may have deposited a contaminate.

4. Kapton tape: used to mask bottom of fuel tray during side wall assembly procedure. The intent of the Kapton tape was to prevent excess RTV from contacting the bottom surface of the fuel tray. Excess RTV could contact the side walls. Kapton tape adhesive may have been deposited on the fuel tray surface.

5. Razor blades: used to remove excess RTV after side wall assembly procedure. The razor was used to cut the excess RTV after it had dried and could have modified the roughness of the surface finish. The visible scratches near the glass side wall are due to the razor blade. (See Figure 4.)

6. Tissues and cotton swabs: used to wipe down fuel tray surfaces with acetone.

3.3 Testing Sources of Contamination

Each of the potential sources of contamination were examined and, when possible, tested.

acetone: The technical grade acetone was a suspected source of contamination from the beginning of the SAL-5 failure review. A technical grade solvent is not very pure. A chemical analysis of the acetone performed by American Testing Company, Inc. (see Attachment A) confirmed the presence of an oily residue and reported "a high level of contamination". *The acetone is a likely source of contamination.*

barrier coating: After each ground-based burn test in the SAL-5 fuel tray, the barrier coating was reapplied to the top of the glass side walls. A cotton swab soaked in technical grade acetone was wiped down the inside surface of the glass wall in order to clean up any excess barrier coating. However, the carrier fluid of the barrier coating in not miscible in acetone and acetone does not remove the barrier coating once it has dried. This cleanup technique likely deposited the excess barrier coating onto the side of the glass walls as well as onto the fuel tray. Small drops of n-butanol placed on the top and side of the glass side wall revealed a uniformly non-wetting surface which is consistent with the presence of barrier coating. In addition, the non-wetting strip discussed in §3.1 is approximately the width of a cotton swab and shows the same wetting characteristics as the side of the glass wall. *The barrier coating is a likely source of contamination.*

silicone RTV: The side walls of the fuel tray were secured using DOW Corning 730 RTV which is a silicone based adhesive. In several locations the RTV was squeezed out of the gap above the bottom of the fuel tray during assembly. A residue may have been left on the areas of the fuel tray surface exposed to the RTV as the RTV solvent evaporated. To test this possibility, RTV was placed on an anodized aluminum sample and allowed to cure. Then a drop of n-butanol was placed in the vicinity of the RTV. In all instances, the n-butanol showed uniform wettability up to the RTV indicating that no solvent residue was present. When

the RTV was pulled from the surface, the wettability of n-butanol was greatly affected in that location. Therefore, a film of the RTV remains after removal, but there is no effect outside the area of adhesion. *The RTV is not a likely source of contamination.*

Kapton tape: Kapton tape was placed on the bottom of the fuel tray during the assembly of the glass side walls so as to prevent excess RTV from contacting the fuel tray surface. It has been determined that any adhesive deposited on the fuel tray surface would be dissolved by either the acetone or the n-butanol during ground-based burn tests and subsequent cleanings. *The Kapton tape is not a likely source of contamination.*

Razor scrapes: The excess RTV which was squeezed out of the gap above the fuel tray surface was removed using a razor blade. The razor blade was placed on the fuel tray surface and pushed into the excess RTV in order to cut the excess off flush with the fuel tray surface. This procedure created scratches in the fuel tray surface perpendicular to the side wall and slightly modified the surface roughness. Although the scratches resulting from the razor blade could pin a contact line, the contamination tests revealed that the non-wetting strip along the edge of the side wall prevented the liquid from contacting the scratches. *The scratches and surface modification resulting from the razor blade are not a likely source of contact line pinning.*

Other materials: Tissue paper was used to wipe out the fuel tray when cleaning. The tissue paper would leave behind lint, but would not deposit any surface contaminating substances. The same is true for the cotton swabs used to wipe down the side walls during cleaning and application of the barrier coating. The tissue paper and cotton swabs could be a vehicle for contamination by the barrier coating and/or the acetone, but there is no substance inherent in the tissues or cotton swabs which would contaminate the surface. *Tissue paper and cotton swabs are not a likely source of contamination.*

3.4 Contamination Summary

The general contamination of the fuel tray is most likely a result of using technical grade acetone to clean the surfaces. A chemical analysis of the acetone used on SAL-5 supports this conclusion. As the acetone evaporates, the non-volatile impurities become more concentrated. Further evaporation results in the acetone film rupturing resulting in wet patches on the fuel tray surface. The impurities in the acetone are distilled in the contact line region and, as the wet patches recede due to evaporation, these impurities are deposited on the fuel tray surface. Additional cleaning of the fuel tray with the acetone results in a buildup of impurities.

Acetone was also used for cleaning excess barrier coating from the side walls. The barrier coating was applied to the top of the glass walls after every ground-based flame test. As a precaution against contamination of the fuel tray by the barrier coating, a cotton swab soaked in acetone was wiped along the side of the each glass wall. Unfortunately, the barrier coating (FC-723, 3M Corp.) is freon based and is immiscible in acetone. It is highly probable that the cotton swab technique actually transferred barrier coating to the fuel tray surface instead of preventing contamination. The width of the high contamination strips is approximately the width of a cotton swab. In addition, the contamination is much more uniform in these strips and on the side of the glass walls than any other location in the fuel tray.

In summary, the process for cleaning the fuel tray is the most probable source of contamination; specifically, the grade of acetone used and the technique for barrier coating cleanup.

4 Mechanical Pump

The mechanical pump must inject the proper amount of fluid into the fuel tray in the correct time. In addition, the liquid must be **one** continuous body in contact with the fuel tray surface and at least one side wall or end wall. The actual liquid volume pumped into the fuel tray must be determined as well as the state of the liquid configuration in the fuel tray.

The flight video indicates that the liquid was introduced into the fuel tray properly; that is, as a continuous body and in contact with the appropriate surfaces. The pump operation and the volume of liquid pumped

have been found to be correct. The details of the mechanical pump evaluation are discussed elsewhere.

5 Filling the Gaps

The side wall attachment process resulted in a gap between the fuel tray and the side wall (see Figure 5). The edge of this gap was very sharp and is an energy barrier to the spreading contact line; that is, the liquid stops spreading when encountering the edge. The contact line becomes pinned on the edge which allows the liquid surface to rotate at the contact line without displacing as the volume of liquid changes. Therefore, as the liquid volume in the fuel tray increases via the mechanical pump, the surface of the liquid can change shape without moving past the pinning edge. The pinning edge is a serious problem for SAL-5 since the liquid will not wick along the sides of the fuel tray unless the gap is filled with liquid. If the liquid does not break over the pinning edge, then the only mechanism for moving liquid down the fuel tray after the mechanical pump is shut off is natural spreading.

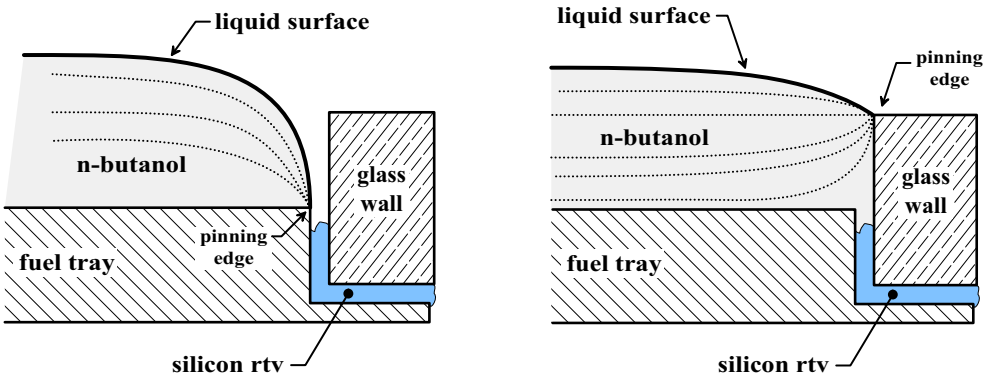

Figure 5. Cross section of SAL-5 fuel tray illustrating the pinning of the contact line. A pinning edge allows the liquid surface to change shape as the volume of liquid increases. In order to fill the fuel tray, the contact line must break past the energy barrier presented by the pinning edge created by the gap. The figure on the left illustrates a contact line pinned at the gap. The figure on the right illustrates the contact line pinned at the top of the glass side wall after the gap has filled with liquid.

The inability to fill the gaps in the fuel tray was noticed during ground-based testing. In response, small pieces of felt were inserted into the gap on one side in order to wick the liquid into that gap. The felt provided a mechanism to overcome the energy barrier presented by the pinning edge. The second gap was too narrow to insert the felt. The narrow gap had filled during ground-based testing and during KC-135 testing and was not considered a risk for flight. The decision to leave the felt out of the narrow gap was not known by all of the SAL-5 team members. It was the gap without the felt inserts which did not fill during the SAL-5 flight and the flight video clearly shows the n-butanol pinning on the edge of the gap.

5.1 Effect of Contamination on Gap Filling

The general, heterogeneous contamination on the bottom of the fuel tray surface slowed the spread of n-butanol, but did not directly effect the ability to fill the gap. However, the non-wetting strips along each side of the fuel tray (see §3.1) did effect the ability to fill the gap. In several locations, the contact line pinned at the non-wetting strip and never reached the edge of the gap. The high contamination along the sides of the fuel tray exacerbated an already difficult situation. Yet, it is unlikely that the gap would have filled even without this contaminated strip.

5.2 Filling the Gaps Summary

To summarize, the failure to fill one gap with n-butanol was due to the design of the fuel tray. The primary factor was the presence of a sharp edge which pinned the contact line of the spreading n-butanol. Contamination found in the non-wetting strip along the sides was an important secondary factor.

6 Corner Flow

The flight video clearly indicates that the redistribution of liquid around the periphery of the fuel tray did not occur as planned. This was due to the inability to fill the gap on one side of the fuel tray. A theoretical analysis of the wicking time based upon capillary flow in a corner was conducted prior to flight for the *anticipated* flight conditions and this analysis predicted that the wicking time would have been acceptable. The analysis and the *anticipated* flight conditions used for the analysis have been examined. In addition, the discrepancies between the conditions used in the analysis and the actual flight conditions have been examined. The most obvious discrepancy is the presence of a gap between each glass side wall and the bottom of the fuel tray.

The original analysis on the corner flows was conducted by Dr. Mark Weislogel, now located at TDA Research, Denver, Colorado. The details of the analysis can be found in NASA TM 107364. A summary of Dr. Weislogel's calculations is presented in Appendix B.2. Dr. Weislogel determined that 147 seconds was required for the liquid to wick a distance of 289 mm. If all of the liquid were in the tray and mounded up at the fill port side so as to double the height from 2 mm to 4 mm, then the wicking time would be reduced to 104 seconds. In addition, if the liquid filled half of the tray and the height was 4 mm, then the wicking time would further be reduced to 26 seconds. Dr. Weislogel's recommendation was to pump all of the liquid into the fuel tray for 60 seconds allowing the liquid to mound up and then allow for another 30 seconds for the fuel tray to fill itself via wicking in the corners. The total fill time required in this scenario is 90 seconds.

The original calculations were verified within the given design parameters; that is, a 0° contact angle and a 90° interior corner (see Appendix B.2). The presence of the gap eliminated the 90° interior corner, but has very little affect on this analysis provided that the liquid fills the gap. Note that the gap is not the barrier, but rather the pinning edge created by the gap is the barrier to filling the gap.

6.1 Effect of Contamination on Corner Wicking

Based upon droplet spreading tests (see §7 for a description of the spreading tests), the actual contact angle was found to be between 5° and 20° due to surface contamination of the fuel tray. The calculations were based on a 0° contact angle. The increase in the contact angle does not significantly affect the wicking time in the corner for contact angles less than 20°. For example, Table 1 shows the effect of contact angle on the time for the tips of the liquid in the corners to meet at the end opposite the fill port based upon a wicking length of 300 mm. Appendix B.2 provides the details of the wicking time calculations. Table 1 also gives the volumetric flow rates for a 300 mm wicking length and various contact angles. Note that once the liquid tips converge at the same location, the flow rate analysis becomes invalid.

6.2 Corner Flow Summary

In conclusion, the original wicking analysis is appropriate. The effect of contamination on the wicking time is manifested in the contact angle and, as seen in Table 1, the wicking time does not change much for contact angles less than 20°. In addition, The presence of the gap does not change the wicking time significantly; provided the liquid fills the gap.

Table 1. Effect of contact angle on tip speed and flow rate of n-butanol in the SAL-5 fuel tray. A wicking length of 300 mm was used for the tip time and the flow rate. The **tip time** is that time required for the tips of the wicking liquid to meet at the end opposite of the fill port. The **flow rate** is the steady volumetric flow rate for a wicking length of 300 mm and an initial liquid surface height of 4 mm. Details of the calculations can be found in Appendix B.2.

contact angle	tip time	flow rate
0°	158 seconds	1.152 cc/min
5°	161 seconds	1.128 cc/min
10°	172 seconds	1.064 cc/min
20°	234 seconds	0.847 cc/min

7 Spreading

The time required for the liquid to wet the bottom of the fuel tray was not considered prior to flight. In order to determine the time required for the liquid to wet the bottom of the SAL-5 fuel tray during flight, a series of spreading tests were conducted. The tests consisted of placing a small drop of n-butanol on an aluminum substrate and measuring the diameter of the wetted surface as a function of time. The surfaces included anodized aluminum of various roughness, non-anodized aluminum surfaces, and the SAL-5 fuel tray. Drop volumes of 3, 5, and 10 μliters were used. Table 5 in Appendix A lists all of the spreading tests conducted in normal gravity. The spreading of 3 and 10 μliter drops on selected surfaces can be seen in Figure 10 in Appendix B.3.

The spread rate of the n-butanol drops was found to follow a power law with two empirically determined spreading coefficients, a and b, which varied with surface finish and degree of contamination. The power law model provides a good predictive tool for the spread of small drops (see Figure 11, Appendix B.3). However, the liquid in the SAL-5 fuel tray was not a spreading drop.

In order to predict the time to wet the bottom of the SAL-5 fuel tray during flight, the drop spreading model (equation 13, Appendix B.3) had to be modified to a planar spreading model. The gravitational acceleration is accounted for in the characteristic time scale, t_s. Using the dimensions of fuel tray and incorporating an aspect ratio of the spreading front, the spreading model for the SAL-5 fuel tray becomes:

$$x = \left(\frac{2hL}{w}\right)\frac{1}{b}\left(\frac{t}{t_s}\right)^a \quad , \tag{1}$$

where x is location of the liquid along the centerline of the SAL-5 fuel tray. The height, width, and length of the fuel tray are h, w, and L, respectively. The characteristic time scale, t_s, is the same as in the drop spreading model (equation 13, Appendix B.3). The spreading parameters, a and b, have the values determined from the drop spreading tests. For the SAL-5 fuel tray surface, these values are $a = 0.40$ and $b = 3.15$ (see Table 4).

The intent of this model is to predict the time required for the liquid to spread completely over the bottom of the fuel tray. Equation 1 is valid for natural spreading only when the pump is not operating. To accurately determine the spreading time, the position of the liquid must be known when the mechanical pump stops. The position of the liquid as it is pumped into the fuel tray can also be determined from Equation 1 by empirically determining the spreading parameters a and b during pump operation. The values of the spreading parameters for pump operation were found to be $a = 0.91$ and $b = 55$. For a positive displacement pump, a should be equal to 1. The mounding up of liquid at the fill port and wicking in the corners result in a value for a slightly less than 1.

The fuel tray spreading model can easily be built as a composite of the different spread rates (see Appendix B.3). Figure 6 illustrates the composite model using the parameters for natural spreading on the fuel tray surface and the parameters for spreading during pump operation. Segment 1 of the model is a natural spread rate for 10 seconds. Segment 2 of the model is a forced spread rate while the mechanical

pump operates. Finally, segment 3 is again the natural spreading rate. The composite model provides an accurate prediction of the centerline location of the liquid front in the SAL-5 fuel tray in low gravity. Using the composite model, the time required for the liquid to spread 298 mm, the length of the fuel tray, would have been nearly 9 minutes.

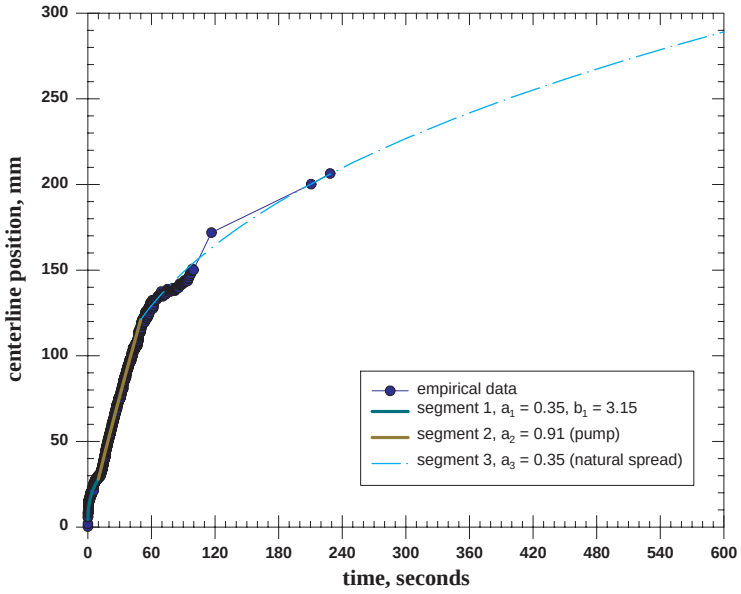

Figure 6. Composite spreading model prediction of the centerline location of liquid in SAL-5 fuel tray.

7.1 Effect of Contamination on Spreading

As described in §3, the SAL-5 fuel tray was found to be contaminated. The effect of contamination on the spreading of n-butanol can be evaluated by estimating the spreading times in the fuel tray using parameters determined for uncontaminated surfaces. The spreading parameters, a and b, were determined from drop spreading tests (see Table 5 in Appendix A). The surface roughness of the SAL-5 fuel tray is similar to the 8/16 rms samples. Table 2 lists the predicted times for n-butanol to spread 100 mm and 200 mm on various aluminum surfaces. A comparison of the fuel tray spread times to the spread times on the 8/16 rms samples indicates that contamination has a significant effect.

7.2 Spreading Summary

The time required for the liquid to spread across the fuel tray was not considered prior to flight. Drop spreading tests and empirical modeling suggest that the spreading time is significant; more so for a contaminated surface. The spreading time is on the order of a few minutes for an uncontaminated, smooth, anodized surface (8/16 rms surface). Contamination increases this spreading time to tens of minutes. Therefore, the liquid would not have spread across the fuel tray surface before the end of the sounding rocket flight even should both gaps have filled with liquid. If there had been no contamination, the liquid may have spread over the fuel tray surface before the end of the flight, but not within the two minutes allocated for the filling sequence.

Table 2. Comparison of model predictions of time required for n-butanol to spread 100 mm and 200 mm on various aluminum surfaces in the SAL-5 fuel tray in low gravity. The spreading parameters, a and b, were determined from drop spreading tests conducted in normal gravity (see Table 5 in Appendix A). Note that these times and spreading distances do not include the spreading due to the mechanical pump and are not predictions of spreading times in the fuel tray during flight.

	parameters		time to spread	
surface type	a	b	100 mm	200 mm
fuel tray	0.40	3.15	128 seconds	724 seconds
8/16 rms, anodized	0.68	22	97 seconds	269 seconds
beadblasted, anodized	0.75	22	41 seconds	123 seconds
beadblasted, unanodized	0.72	7	13 seconds	34 seconds

8 Leveling

The time required for the liquid to minimize its surface shape, or level should the volume of liquid be correct, was not considered before the flight. In a low-gravity environment, the only mechanism to level a liquid surface is a capillary pressure which arises from surface curvature. The initial change in surface shape occurs rapidly. But, as the liquid surface flattens, the capillary driving pressure goes to zero which results in a slowing of surface reorientation. If the liquid system is inertial dominated, the momentum of the liquid can help in leveling the surface. However, if the liquid system is viscous dominated, then the liquid quickly ceases to flow as the capillary pressure diminishes. Thus, for a viscous system, the leveling time could be quite long.

An estimate of the leveling time can be obtained from Burelbach, Bankoff, and Davis (1988) who developed an evolution equation for the interface shape of a thin liquid film subjected to perturbations (see Appendix B.4). The time, in seconds, for the surface to level can be approximated as:

$$t \sim \frac{3\mu}{\sigma}\frac{x^4}{h^3} \quad , \tag{2}$$

where x is the length of the liquid surface and h is the mean liquid thickness. Using the properties on n-butanol at room temperature and a tray height of 2 mm, the leveling time for various surface lengths is given in Table 3. Note that these times are accurate only to an order of magnitude and represent an upper limit on the leveling time in the fuel tray.

Table 3. Settling times of the liquid surface with an average height of 2 mm. These times are only accurate to an order of magnitude.

liquid surface length	settling time
half-width of tray, 40 mm	115 seconds
width of tray, 80 mm	31 minutes
half-length of tray, 150 mm	6 hours
length of tray, 300 mm	101 hours

The leveling times in Table 3 appear to be excessively long. The initial reorientation of the liquid surface may be quite rapid, i.e., a few seconds; whereas the last 5 to 10% of leveling may take 90% of the time. The evolution profile can only be determined numerically.

8.1 Effect of Contamination on Leveling

Contamination of the fuel tray surfaces was not a factor in the settling time calculation for the SAL-5 liquid surface.

8.2 Leveling Summary

Based upon this analysis, it is unlikely that the SAL-5 liquid surface would have been level at ignition. However, degree of level at ignition is not known. Also, the flatness requirement for the SAL-5 liquid surface is not specified. Therefore, it is uncertain if the leveling time would have been a limiting condition in proper filling of the fuel tray.

9 Conclusion

The experimental and analytical efforts described in §3 through §8 was conducted in order to answer the questions posed in §2. The questions are reiterated here in order to summarize the findings.

1. Why did the liquid not fill the gap on one side?

   The gap provided a pinning edge which prevented the liquid from touching the side walls. Capillary flow cannot occur in this system unless the liquid touches both the bottom and the side of the tray[†]. The presence of felt in one gap of the tray allowed for wicking on that side. However, the gap without the felt did not fill and the liquid remained pinned on the edge of the fuel tray. The non-wetting contaminated strips along each side of the fuel tray did effect the ability to fill the gap. In several locations, the contact line pinned at the non-wetting strip and never reached the edge of the gap. It is unlikely, though, that the gap would have filled even without this contaminated strip. To summarize, the failure to fill one gap with n-butanol was due to the design of the SAL-5 fuel tray. The primary factor was the presence of a sharp edge which pinned the contact line. Contamination found in the non-wetting strip along the sides was an important secondary factor.

2. Assuming that both gaps had filled with liquid, would the fuel tray have filled properly in the allotted time?

   No. The correct volume of liquid was introduced into the fuel tray and the original wicking analysis was correct. However, the spreading and leveling times were much too long for a sounding rocket flight. The time required for the liquid to spread 150 mm (half of the fuel tray length) was nearly 6 minutes. The long spreading time can be attributed to contamination of the fuel tray. The detrimental effect of contamination gives rise to another question.

3. Assuming both gaps had filled with liquid and there was no contamination, would the fuel tray have filled properly in an *acceptable* time?

   The total time required for filling can be determined by summing the estimates of each of the fill events:

mechanical pump time	60 seconds
wicking time	—
spreading time	125 seconds
leveling time	20 seconds
	205 seconds

   The wicking time is not included because the corner wicking occurs at the same time as spreading and spreading is the limiting case; that is, spreading takes longer than does the corner wicking. The predicted spreading time is for the 8/16 rms anodized aluminum surface parameters ($a = 0.68$ and

[†] The static contact angle must also be below a critical value, but this is not an issue for SAL-5.

$b = 22$). The leveling time is estimated to be 20 seconds for the surface to reach a suitable degree of flatness. Therefore, the total time to fill the SAL-5 fuel tray is approximately 200 seconds. Since the time calculations are approximate, the actual fill time may be closer to 3 minutes or as long as 6 minutes. The total low-gravity time provided by the sounding rocket is 4 to 6 minutes. It is uncertain if the fuel tray would have filled in time to conduct the experiment based solely upon these calculations.

An additional factor must be taken into account. The through-holes in the fuel tray for the three thermocouples had a sharp edge at the fuel tray surface (see Figure 7 in Appendix A for thermocouple locations). As the liquid spread across the fuel tray during flight, the contact line pinned on the sharp edge of these thermocouple through-holes. The momentum provided by the mechanical pump forced the liquid over the pinning edge at the thermocouple nearest the fill port. The center thermocouple had not wetted by the time the ignitor was turned on and the liquid did not reach the thermocouple near the ignitor until the sounding rocket began to spin-up for reentry. It is unlikely that the liquid would have wetted the ignitor thermocouple. It is also probable that the center thermocouple would not have been wetted had the filling process gone as planned. Therefore, the SAL-5 experiment would not have filled properly in an acceptable time during flight even if both gaps had been filled and there was no contamination.

It is my opinion that the primary cause of the failure to fill properly is the geometry of the fuel tray; that is, the presence of the gaps on the side walls and the sharp edge around the thermocouple through-holes. The contamination resulting from the cleaning process is a strong secondary factor which would have prevented proper, timely filling had the primary cause not been present.

9.1 Additional Comments Concerning Fill Process

Several fill and ignition tests were conducted in low-gravity aircraft prior to the SAL-5 flight. These low-gravity tests indicated that filling the fuel tray would not be a problem. However, these aircraft tests could have been very misleading. The low-gravity aircraft facilities provide a nominal environment of 10^{-2} to 10^{-3} g-level for 15 to 20 seconds, but there is a great deal of vibration associated with this nominal environment. The vibrations on the aircraft, both mechanical and acoustical, are capable of moving the liquid around the fuel tray. The aircraft vibrations could assist the filling of the fuel tray by:

- providing momentum to overcome the pinning energy at the gap edge;
- imparting momentum to the liquid to assist with spreading; and
- imparting momentum to the liquid to assist with leveling.

A liquid surface is extremely sensitive to vibrations and great care should be taken when interpreting capillary phenomena observed on low-gravity aircraft.

Although great care was taken in many aspects of the SAL-5 design and fabrication, there was a general lack of understanding of chemical purity and compatibility. The SAL-5 team members were not aware of what is meant by "Technical Grade" solvents and the level of purity associated with this grade. In addition, the miscibility of acetone with the barrier coating was never investigated. It was simply assumed that acetone would clean up the barrier coating. The proper curing and cleanup of the barrier coating was never studied. The lack of knowledge with respect to solvents is due to the perceived irrelevance to the science objectives of flame spread. The inattention to solvents is directly responsible for the contamination of the fuel tray.

Both the misinterpretation of low-gravity aircraft tests and the solvent issues *may* have been avoided had there been a coordinated design review. All members of the SAL-5 team, science and engineering, were not informed as design decisions were made and implemented. Some blame lies in the turnover of project personnel and managers, but the majority of the blame lies in a lack of engineering discipline. Design reviews were not held and engineering changes were poorly documentation if at all. An example of the resulting miscommunication is the science team did not know until after the flight that felt was not inserted into both gaps. Another example is the absence of an up-to-date electrical schematic. The direct mechanisms

of failure can be attributed to the design of the fuel tray and contamination, but I strongly feel that the cause of failure is programmatic. Project and design reviews as well as better engineering discipline may have prevented the failure of the SAL-5 experiment.

10 References

Burelbach, J. P., Bankoff, S. G., and Davis, S. H., "Nonlinear stability of evaporating/condensing liquid films", J. Fluid Mech. (1988), vol. 195, pp. 463–494.

Weislogel M.M., "Capillary Flow in an Interior Corner", NASA Technical Memorandum 107364, Nov. 1996.

A Data Tables

Table 4. Locations of contamination tests performed on the SAL-5 fuel tray. Figure 7 illustrates the location of the test points in the fuel tray.

test #	drop coordinates x	drop coordinates y	drop volume	estimated contact angle	notes
1	31	4	1 μliter, 1 time	5 to 10°	non-uniform wetting, distorted contact line
2	92	50	1 μliter, 3 times	5 to 10°	non-uniform wetting
3	62	5.3	1 μliter, 4 times	5 to 10°	non-uniform wetting, zoomed in twice
3b	70	15	1 μliter, 3 times	5 to 10°	arbitrary location, non-wetting patches large scratch which does not wick
4	89	22	4 μliters, 2 times	5 to 10°	not recorded on video
5	108	35	10 μliters, 3 times	5 to 10°	non-uniform wetting
6	112	50	10 μliters, 2 times	5 to 10°	large dimple at non-wetting patch
7	105	0	10 μliters, 3 times	10 to 20°	forced liquid to edge on 3rd drop shows scratches in edge
8	23	5.3	not tested		too close to tests 1 and 9
9	31	0	10 μliters, 3 times	10 to 20°	forced liquid to edge of tray large dimples in contact line area
10	120	80	1 μliter, 1 time	$> 20°$	non-wetting strip near wall
11	130	80	1 μliter, 1 time	$> 20°$	non-wetting strip near wall
12	20	80	1 μliter, 1 time		irregular drop shape
13	40	80	1 μliter, 1 time		irregular drop shape
14	60	80	1 μliter, 1 time		irregular drop shape
15	80	80	1 μliter, 1 time		irregular drop shape
16	90	80	1 μliter, 2 times		irregular drop shape
17	210	80	1 μliter, 1 time		irregular drop shape
18	210	70	1 μliter, 1 time		irregular drop shape
19	220	80	4 μliters, 1 time		non-wetting spot near wall
20	120	70	10 μliters, 3 times 5 μliters, 1 time 4 μliters, 1 time 25 μliters, 1 time		drop does not wet a strip near wall pointing at non-wetting patches in video 64 μliters total
21-36	top of glass		1 μliter each	$> 45°$	drop location on non-felt side: 1, 3, 5, 6, 7, 9, 11, 13, 15, 17, 19, 21, 23, 25, 27 cm drop location on felt side: 26, 24 (2 μliters), 22, 20, 18.5, 16, 14, 12 cm drop location on end walls: 1 drop on ignitor end, 1 drop on fill port end
37-38	ign. brackets		1 μliter each	$< 1°$	wetting
39-50	side of glass		1 μliter each	20 to 45°	drop location on non-felt side: 1.5, 4, 8, 10, 12.5, 14, 19, 23, 25, 28, 29 cm

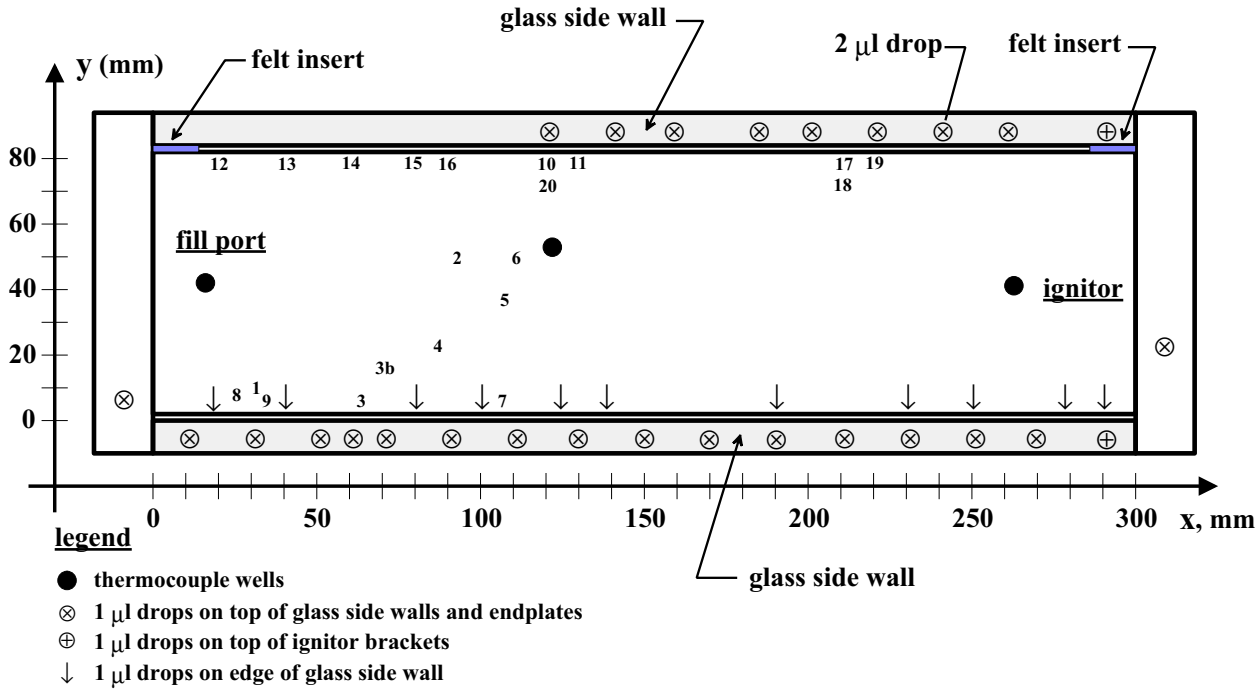

Figure 7. Layout of SAL-5 fuel tray indicating location of contamination test points listed in Table 4.

Table 5. Drop spreading tests conducted for SAL-5 failure review board. Various volumes of n-butanol were placed on aluminum and glass substrates in order to examine the effect of surface roughness and anodization on wettability.

data set	test sample	drop volume (μliters)	final radius (mm)	calculated contact angle (deg)	spreading parameters a	spreading parameters b	notes
d1	8 rms	10	8.8	1.86	0.68	22	drop fell $\sim$ 5 mm
d2	16 rms	10	8.9	1.81	0.68	22	drop fell $\sim$ 5 mm
d3	32 rms	10	8.3	2.14	0.54	8	irregular drop shape
d4	beadblast, anod.	10	11.4	1.02	0.75	22	drop fell $\sim$ 5 mm
d5	fueltray	10	7.2	3.00	0.4	3.15	drop near ignitor, irreg. shape
d6	fueltray	10	7.9	2.40			drop near center thermocouple, irregular shape
d7	beadblast sample 1	10	13.9	0.66	0.77	22	
d8	beadblast sample 2	10	13.7	0.68	0.81	22	measured data cut off too soon
d9	beadblast sample 3	10	11	1.11	0.73	22	
d10	beadblast sample 4	10	8.8	1.86			drop follows grain of sample
d11	beadblast sample 3	10	10.9	1.13			sample washed
d12	beadblast sample 4	10	7.6	2.64			sample washed
d13	beadblast sample 4	10					tested on non-beadblasted side
d14	beadblast sample 4	10					sample washed, tested on non-beadblasted side
x1	32 rms	3					bad experiment run

continued on next page

Table 5. (continued)

data set	test sample	drop volume (μliters)	final radius (mm)	calculated contact angle (deg)	spreading parameters a	spreading parameters b	notes
x1-2	32 rms	3	4.94	2.33	0.5	7.5	second tracking of data
x2	32 rms	3	3.75	4.86			
x3	16 rms	3	6.1	1.36	0.55	6.5	
x4	16 rms	3					
x5	8 rms	3	5.53	1.74	0.6/0.68	11/22	
x6	8 rms	3					
x7	beadblast, non-anod.	3					
x8	beadblast, non-anod.	3	8.8	0.56			questionable tracking data
x8-2	beadblast, non-anod.	3	8.67	0.58	0.72	7	second tracking of data
x9	beadblast, non-anod.	3					pulled drop with syringe
x10	beadblast, non-anod.	3	9	0.53	0.8	14	
x11	16 rms	3					possible contamination
x12	16 rms	3					possible contamination
x13	32 rms	5	6.5	1.93			
x14	32 rms	5					
x15	16 rms	5					definite contamination
x16	16 rms	5	5.56	2.86			definite contamination
x17	8 rms	5	6.2	2.17			
x18	8 rms	5	4.66	4.52			
x19	beadblast, anod.	5	5.28	3.27			tracker rad. $\ll$ manual rad.
x20	beadblast, anod.	5	4.83	4.12			didn't include hazy fringe, resulted in a smaller rad.
x20-2	beadblast, anod.	5	5.26	3.30	0.45	8.75	2nd tracking of data, incl. hazy area, irregular shape
x20-3	beadblast, anod.	5	5.17	3.45			3rd tracking of data, incl. hazy area, irregular shape
x21	beadblast, non-anod.	5	10.2	0.66	0.72	11	
x22	beadblast, non-anod.	5					
x23	16 rms	10	4.9	7.90			possibly contaminated
x24	16 rms	5	4.03	6.65			
x25	16 rms	5	4.18	6.03			
x26	beadblast, anod.	3	4.66				
x27	beadblast, anod.	3					visible rings at end of test
x28	8 rms	5	3.75	8.06			sample cleaned
x29	glass slide	5					possibly contaminated
x30	glass slide	5	3.71	8.30	0.29	1.15	possibly contaminated
x31	beadblast, anod.	3	4.58	2.84			drop placed inside of visible ring
x31-2	beadblast, anod.	3	4.84	2.46	0.43	3.75	2nd tracking of data, tracker rad. $\ll$ manual rad.

continued on next page

Table 5. (continued)

data set	test sample	drop volume (μliters)	final radius (mm)	calculated contact angle (deg)	spreading parameters a	b	notes
x32	beadblast, anod.	3	4.6	2.81			drop inside of both visible rings
x33	beadblast, anod.	3					drop centered on edge of ring

B Calculations

B.1 Contact Angle Determination

The static contact angle can be determined using the measured wetted diameter of the solid surface and the known volume of the drop as boundary conditions. Figure 8 illustrates the geometry used for the analysis. The pressure drop across the liquid-vapor interface is a function of gravitational potential and capillary pressure. Therefore,

$$P_v - P_l = \sigma \left(\frac{1}{R_1} + \frac{1}{R_2} \right) = (\rho_l - \rho_v) g y + c \quad . \tag{3}$$

The various parameters are defined as:

P_v	vapor pressure	ρ_v	vapor density
P_l	liquid pressure	ρ_l	liquid density
σ	surface tension	R_1, R_2	radii of curvature of drop
g	gravitational acceleration	c	unknown constant

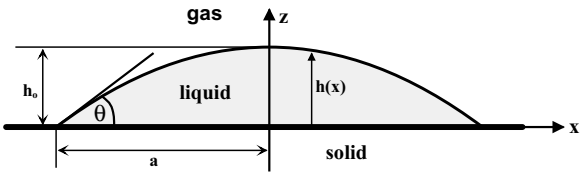

Figure 8. Static drop on smooth surface. a is the radius of the wetted surface, h is the drop height, and θ is the static contact angle.

Explicit expressions for the two radii of curvature, R_1 and R_2, can be obtained because the drop is a figure of revolution. The radius of the wetted surface, a, will be used to non-dimensionalize equation 3 because this radius is a measured parameter. Dimensionless length scales are defined as:

$$\eta = \frac{h}{a} \qquad \text{and} \qquad \xi = \frac{x}{a} \quad . \tag{4}$$

A modified Bond number is defined to be:

$$\boxed{\beta \equiv \frac{a}{L_c}} \quad \text{where } L_c \text{ is the capillary length, } \boxed{L_c \equiv \sqrt{\frac{\sigma}{\Delta \rho g}}} \quad . \tag{5}$$

The dimensionless parameter, β, is a variation of the Bond number. Normally, the length scale, a, would be a poor characteristic length for a Bond number since it is perpendicular to the gravity vector. However, for this analysis a is a useful length scale because it is known. The drop is assumed to isothermal so there is no variation in surface tension, σ.

Substituting the dimensionless parameters into equation 3 results in the following differential equation:

$$\frac{\eta''}{(1+\eta'^2)^{3/2}} + \frac{\eta'}{\xi(1+\eta'^2)^{1/2}} = \beta^2 \eta + \overline{c} \quad . \tag{6}$$

The prime notation indicates the derivative with respect to ξ.

The slope of the drop is assumed to be small which is equivalent to small static contact angles, θ. The small slope approximation will be valid when $\tan\theta^2 \ll 1$ which limits θ to less than 20°. Using the small slope approximation significantly reduces the complexity of equation 6. Further simplification is obtained by transforming, ξ and η. The result is a zeroeth order, modified Bessels equation. The solution to which is

$$\eta = \frac{1}{\beta^2}\left\{\alpha_1 \mathrm{K}_0(\beta\xi) + \alpha_2 \mathrm{I}_0(\beta\xi) - \overline{c}\right\} \quad , \tag{7}$$

where K_0 and I_0 are modified Bessels functions. There are three unknown constants ($\overline{c}$, α_1, and α_2) which will be determined two different sets of boundary conditions.

Applying the appropriate boundary conditions results in an expression for the interface shape when the wetted diameter, $2a$, and the drop volume, V, is known:

$$\eta(\xi) = \frac{V^*}{\beta^2}\left[\frac{\mathrm{I}_0(\beta\xi) - \mathrm{I}_0(\beta)}{2\,\mathrm{I}_1(\beta) - \beta\,\mathrm{I}_0(\beta)}\right] \quad , \tag{8}$$

where V^* is a dimensionless volume defined as

$$\boxed{V^* \equiv \frac{V}{\pi {L_c}^3}} \quad . \tag{9}$$

Again, the solution shown in equation 8 is valid for static contact angles, θ, less than 20°.

The tangent of the static contact angle is the slope of the drop at the contact line; that is, $\tan\theta = \eta'(1)$. Taking the derivative of equation 8 and setting ξ equal to 1 allows for an explicit expression for the static contact angle as a function of wetted diameter and the volume of the drop,

$$\boxed{\tan\theta = \frac{V^*}{\beta}\left[\frac{\mathrm{I}_1(\beta)}{\beta\,\mathrm{I}_0(\beta) - 2\,\mathrm{I}_1(\beta)}\right] \quad \text{for } 0 < \theta < 20^\circ} \quad . \tag{10}$$

Figure 9 illustrates the dependence of contact angle on drop volume and wetted diameter.

B.2 Corner Flow Time

The original analysis of the corner flow was conducted by Dr. Mark Weislogel, now at TDA Research in Denver, Colorado. The development of the theory is presented in NASA TM 107364, "Capillary Flow in an Interior Corner", November 1996. Using the geometry of the fuel tray, the fluid properties on n-butanol at room temperature, and a 0° contact angle, Dr. Weislogel determined that the wicking time, t, in the SAL-5 fuel tray is related to wicking length, $\mathcal{L}$, by

$$t = 1763\mathcal{L}^2 \quad , \tag{11}$$

where t is in seconds and $\mathcal{L}$ is in meters. For $\mathcal{L}$ equal to 0.289 m, the wicking time is 147 seconds. Doubling the height of the liquid surface from 2 mm to 4 mm provides additional capillary pressure which reduces the wicking time by

$$t = \frac{147}{\sqrt{2}} = 103.9 \text{ seconds.} \tag{12}$$

Further, if $\mathcal{L}$ is reduced by half, the wicking time is reduced by a factor of 4. The wicking time then reduces to 26 seconds. Based upon these calculations, Dr. Weislogel recommended that all of the liquid be pumped into the fuel tray during the first 60 seconds. The average liquid surface height would be 4 mm assuming the liquid filled half of the fuel tray. The next 30 seconds would wick the liquid down the corners. The total fill time would be 90 seconds.

Dr. Weislogel's calculations were duplicated for contact angles other than 0° with a 2 mm liquid surface height and are presented in Table 6. The influence of contact angle is found to be relatively insignificant

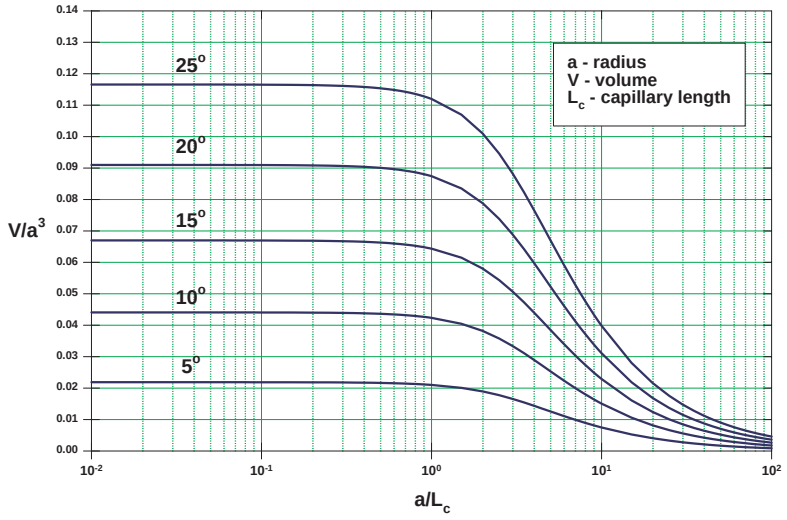

Figure 9. Contour plot of static contact angle as a function of the wetted radius, a, the drop volume, V, and the modified Bond number, β. The modified Bond number is defined as $\beta = a/L_c$ where L_c is the capillary length and is defined as $\sqrt{\sigma/\rho g}$.

for angles less than 20°. The general contamination of the fuel tray surface does not appear to affect the wicking time. The strip of high contamination along each side wall may have had significant effect were there no gap. The presence of the gap may have offset the effect of the high contamination strip by providing an alternate wicking mechanism to that of an interior corner.

Table 6. Expressions for wicking time as a function of wicking length, $calL$ and static contact angle. The nominal liquid height is 2 mm.

contact angle	wicking time	$\mathcal{L} = 0.3$ m	$\mathcal{L} = 0.15$ m
0°	$t = 1756\,\mathcal{L}^2$	158 seconds	39.5 seconds
5°	$t = 1789\,\mathcal{L}^2$	161 seconds	40.3 seconds
10°	$t = 1912\,\mathcal{L}^2$	172 seconds	43.0 seconds
20°	$t = 2597\,\mathcal{L}^2$	234 seconds	58.4 seconds

B.3 Spreading Time

In order to determine the time required for the liquid to wet the bottom of the SAL-5 fuel tray during flight, a series of spreading tests were conducted. The tests consisted of placing a small drop of n-butanol on an aluminum substrate and measuring the diameter of the wetted surface as a function of time. The surfaces included anodized aluminum of various roughness, non-anodized aluminum surfaces, and the SAL-5 fuel tray. Drop volumes of 3, 5, and 10 μliters were used. Table 5 in Appendix A lists all of the spreading tests conducted in normal gravity.

Figure 10 shows the spreading of 3 and 10 μliter drops on selected surfaces. Typically, the wetted radius grows very rapidly during the first few seconds after deployment. This rapid growth stage is due to surface tension reshaping the drop and inertia. The inertia is damped very quickly and the wetted radius then increases at a slower rate. This slower growth is the "natural" spread rate of the drop. After a period of 30

to 40 seconds, the n-butanol begins to evaporate and the wetted radius decreases. The intent of the these tests was to provide empirical data for developing a spreading model which could be used to predict the time to wet the SAL-5 fuel tray. In developing the model, it is assumed that the effects of evaporation are not significant until the wetted radius begins to decrease.

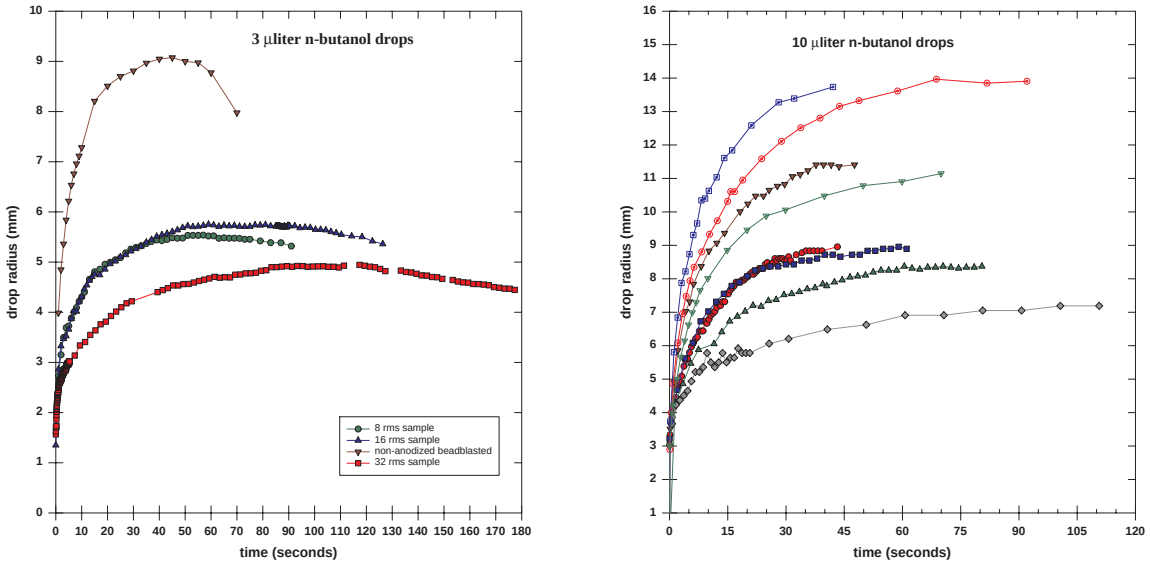

Figure 10. Radius of wetted surface versus time for 3 and 10 μliter drops of n-butanol on various aluminum surfaces. The 8 rms and 16 rms samples are similar in surface roughness. As the drops begin to evaporate, the wetted radius begins to decrease.

The spread rate of the n-butanol drops was found to follow a power law when the wetted radius is non-dimensionalized with volume. The model is

$$\frac{V}{r^3} = b\left(\frac{t}{t_s}\right)^{-a} \quad , \tag{13}$$

where V is the volume of the drop, r is the radius of the wetted surface, t_s is the characteristic time, and a and b are empirically determined spreading parameters. The values of the empirically determined spreading parameters, a and b, are listed in Table 5, Appendix A[‡]. The characteristic time, t_s, represents the time required for the interface to adjust its shape and is a balance between viscous dissipation and capillary pressure.

$$t_s = \frac{3\mu}{\sigma} L_s \quad , \tag{14}$$

where μ is the absolute viscosity, σ is the surface tension, and L_s is the characteristic length scale. The true characteristic time scale for spreading will probably include a squared aspect ratio of the spreading region.

The length scale, L_s, is critical. Generally for a sessile drop, the length scale is set equal to 1/3 of the volume. This form of L_s would make it difficult to correlate the drop spreading parameters, a and b, to spreading in the fuel tray in low gravity. Therefore, the characteristic length scale will be defined as the capillary length,

$$L_s = \sqrt{\frac{\sigma}{\rho g}} \quad , \tag{15}$$

[‡]An interesting sidenote, the spreading parameter b has a value of 22 for n-butanol on clean, anodized aluminum for most surface roughnesses.

where ρ is the liquid density and g is the gravitational acceleration. For the sessile drops in normal gravity, $L_s = 1.76$ mm which results in a characteristic time of $t_s = 6.3 \cdot 10^{-4}$ sec.

Figure 11 illustrates the dimensionless radius versus time and the spreading model predictions of equation 13 for two surface types. The first is for the 8 and 16 rms samples ($a = 0.68$,$b = 22$) and the second is for the contaminated fuel tray surface ($a = 0.40$, $b = 3.15$). The spreading model remains accurate until the evaporation of the drop begins to shrink the wetted radius.

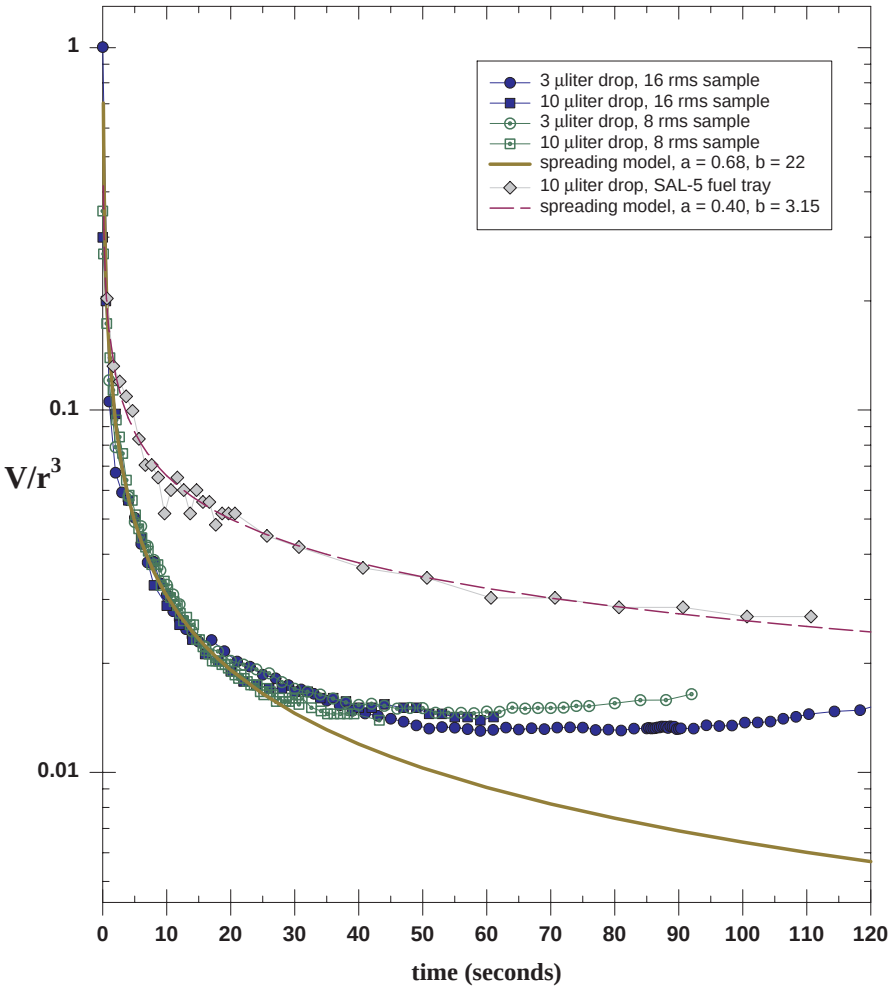

Figure 11. Dimensionless radius, V/r^3, versus time for 3 and 10 μliter drops of n-butanol on 8/16 rms samples and for a 10 μliter drop on the SAL-5 fuel tray. The spreading model is accurate until the drop begins to evaporate.

The liquid in the SAL-5 fuel tray did not spread in the shape of the drop and was not in a normal gravity environment. In order to predict the time to wet the bottom of the SAL-5 fuel tray during flight, the drop spreading model (equation 13) had to be modified to a planar spreading model. Using the dimensions of fuel tray and incorporating an aspect ratio of the spreading front, the drop spreading model was modified

for the SAL-5 fuel tray to be:

$$x = \left(\frac{2hL}{w}\right)\frac{1}{b}\left(\frac{t}{t_s}\right)^a \quad , \tag{16}$$

where x is location of the liquid along the centerline of the SAL-5 fuel tray. The height, width, and length of the fuel tray are h, w, and L, respectively. The gravitational acceleration is accounted for in the characteristic time scale, t_s. The gravitational level used in the length scale (equation 15) is $10^{-4}g$ which resulted in $L_s = 176$ mm and $t_s = 0.063$ seconds. The length scale, L_s, and subsequently the time scale, t_s, are very sensitive to the acceleration level.

The spreading model for the SAL-5 fuel tray was verified by comparing the predicted spread rate to the actual spread rate observed during the flight. Figure 12 shows the centerline location of the liquid during the SAL-5 experiment. The mechanical pump forces the liquid into the fuel tray during the first 60 seconds. The natural spreading begins after the pump has stopped. The spreading parameters, a and b, used in equation 16 have the values determined from the droplet tests conducted on the fuel tray surface. These values are $a = 0.40$ and $b = 3.15$.

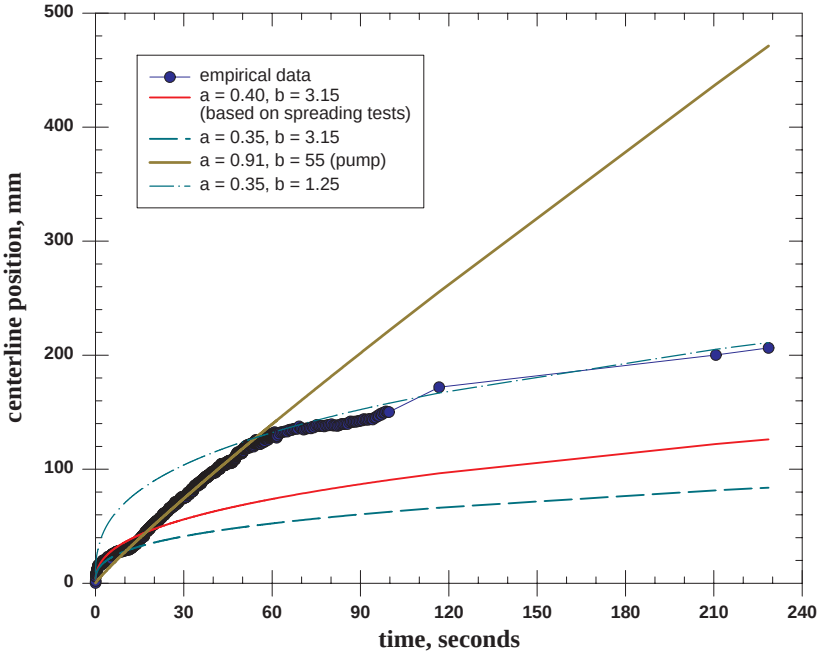

Figure 12. Centerline location of liquid in SAL-5 fuel tray during flight and spreading model predictions.

Four sets of spreading parameters are shown in Figure 12. The first ($a = 0.40$, $b = 3.15$) is based upon the drop spreading test conducted in the fuel tray. The second ($a = 0.35$, $b = 3.15$) is slightly modified to give a better approximation. The reduction in slope, 0.35 versus 0.40, is due to the presence of the thermocouple wells in the center of the fuel tray. The liquid front would temporarily pin on these locations effectively reducing the spreading rate. The third model prediction ($a = 0.91$, $b = 55$) is a fit to the spread rate while the mechanical pump is operating. Normally, the value of a would be 1 for a positive displacement pump. The value of 0.91 occurs because the liquid is mounding up near the fill port and some of the liquid is wicking in the corners. The mounding and wicking of liquid reduces the spread rate along the centerline. The fourth approximation ($a = 0.35$, $b = 1.25$) is a modification of the second approximation and accounts

for the advanced location of the liquid when natural spreading begins; i.e. the location of the liquid when the pump is stopped.

The fuel tray spreading model can easily be built as a composite of the different spread rates. Figure 13 illustrates the composite model using the parameters for natural spreading on the fuel tray surface and the parameters for spreading during pump operation. Segment 1 of the model is a natural spread rate for 10 seconds. Segment 2 of the model is a forced spread rate while the mechanical pump operates. Finally, segment 3 is again the natural spreading rate. The composite model provides an accurate prediction of the centerline location of the liquid front in the SAL-5 fuel tray in low gravity.

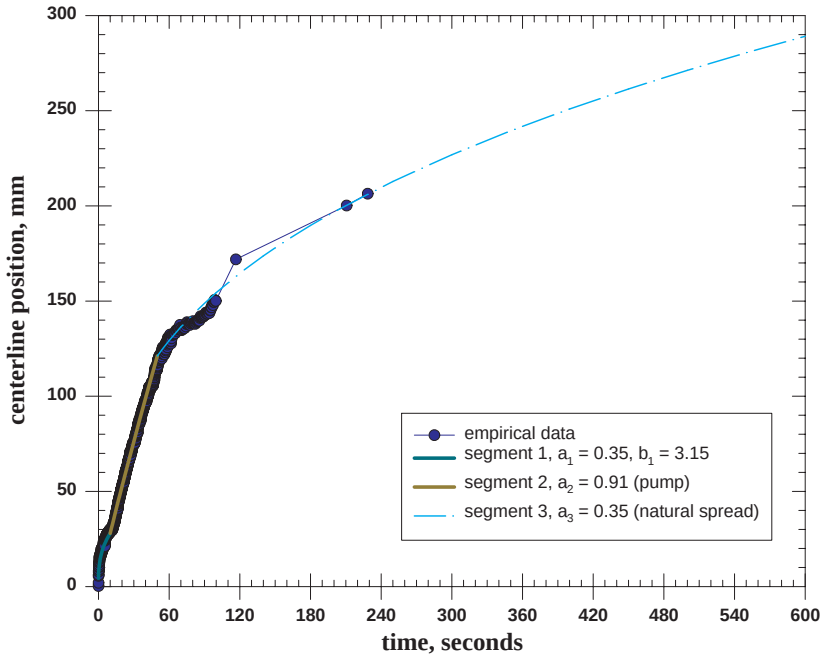

Figure 13. Composite spreading model prediction of location of liquid in SAL-5 fuel tray.

The spreading time for an uncontaminated surface can be estimated by using the composite model and the spreading parameters determined from drop spreading on surfaces other than the fuel tray. Figure 14 illustrates the spreading predictions for the fuel tray surface and for a surface similar to the 8 and 16 rms anodized samples. The mechanical pump is operated for 60 seconds and then the predicted centerline location for spreading on each of the surface types is shown. The spreading rate parameter for the pump ($a = 0.91$) is assumed to be the same for both surfaces. The 8 and 16 rms samples are chosen for comparison because of the similarity in roughness to the fuel tray surface. The effect of contamination on the spread rate is evident in Figure 14. The time required for the liquid to be pumped and to spread a distance of 300 mm is reduced from over 11 minutes on the contaminated surface to 3 minutes on the uncontaminated surface.

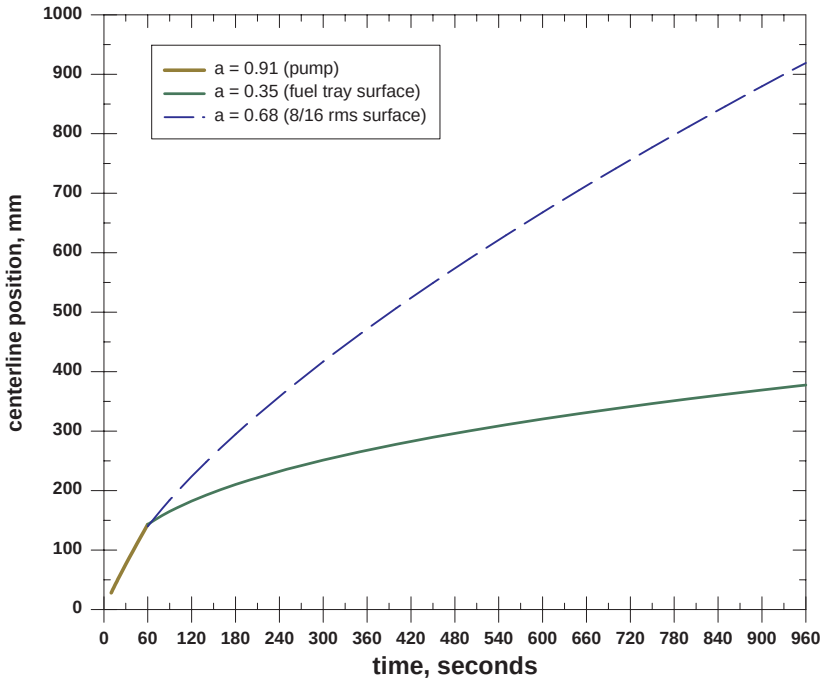

Figure 14. Spreading model predictions for contaminated SAL-5 fuel tray surface and for the uncontaminated 8/16 rms anodized aluminum sample surfaces.

B.4 Leveling Time

In a low-gravity environment, the only mechanism to level a liquid film is capillary pressure which arises from surface curvature. The initial change in surface shape occurs rapidly. But, as the liquid surface flattens, the capillary driving pressure goes to zero which results in a slowing of surface reorientation. The rate of change of the surface shape can be determined through a stability analysis. The stability of liquid films was examined for a variety of conditions by Burelbach, Bankoff, and Davis, J. Fluid Mech. (1988), vol. 195, pp. 463–494. The conditions pertinent to the SAL-5 experiment would be the isothermal film analysis. The resulting nonlinear evolution equation governing long-wave surface disturbances is:

$$\frac{\delta\eta}{\delta\tau} = \mathcal{A}\frac{\delta}{\delta\xi}\left(\frac{1}{h}\frac{\delta\eta}{\delta\xi}\right) + \mathcal{S}\frac{\delta}{\delta\xi}\left(\eta^3\frac{\delta^3\eta}{\delta\xi^3}\right) = 0 \quad , \tag{17}$$

where η is the surface height normalized by the average liquid depth, h, and τ is time normalized by the viscous time scale h^2/ν. The van der Waals parameter, $\mathcal{A}$, is on the order of 10^{-9} for a 2 mm layer of n-butanol. Subsequently, the second term of equation 17 will be neglected. The surface tension parameter, $\mathcal{S}$, is defined as

$$\mathcal{S} = \frac{\sigma}{3\mu}\frac{\rho h}{\mu} \quad , \tag{18}$$

where σ, μ, and ρ are surface tension, absolute viscosity, and density, respectively.

Scaling equation 17 results in the following expression for leveling time:

$$\tau \sim \frac{1}{\mathcal{S}}\frac{\xi^4}{\eta^3} \quad . \tag{19}$$

Dimensionalizing equation 19 results in an order of magnitude estimate of the leveling time:

$$t \sim \frac{3\mu}{\sigma}\frac{x^4}{h^3} \quad , \tag{20}$$

where x is the length of the liquid surface and h is the mean liquid thickness. Based on equation 20, the reorientation time for n-butanol in the SAL-5 fuel tray ($h = 2$ mm, $x = 300$ mm) is 101 hours. This time appears to be excessively long and is indicative of the viscous behavior of the SAL-5 system. Again, these times are strictly order of magnitude estimates and can be misleading. The initial reorientation of the liquid surface may be quite rapid, i.e., a few seconds; whereas the last 5 to 10% of leveling may take 90% of the time. The evolution profile can only be determined numerically which is beyond the scope of this review.

The reorientation time can be significantly decreased by slightly increasing the depth of the fuel tray. For example, increasing the depth of the fuel tray from 2 mm to 3 mm decreases the reorientation time from 101 hours to 30 hours. Increasing the depth to 4 mm decreases the reorientation time to 13 hours. Figure 15 illustrates the relationship between reorientation time and tray depth for n-butanol with a liquid surface length is 300 mm. Reiterating, the reorientation times are only accurate to an order of magnitude.

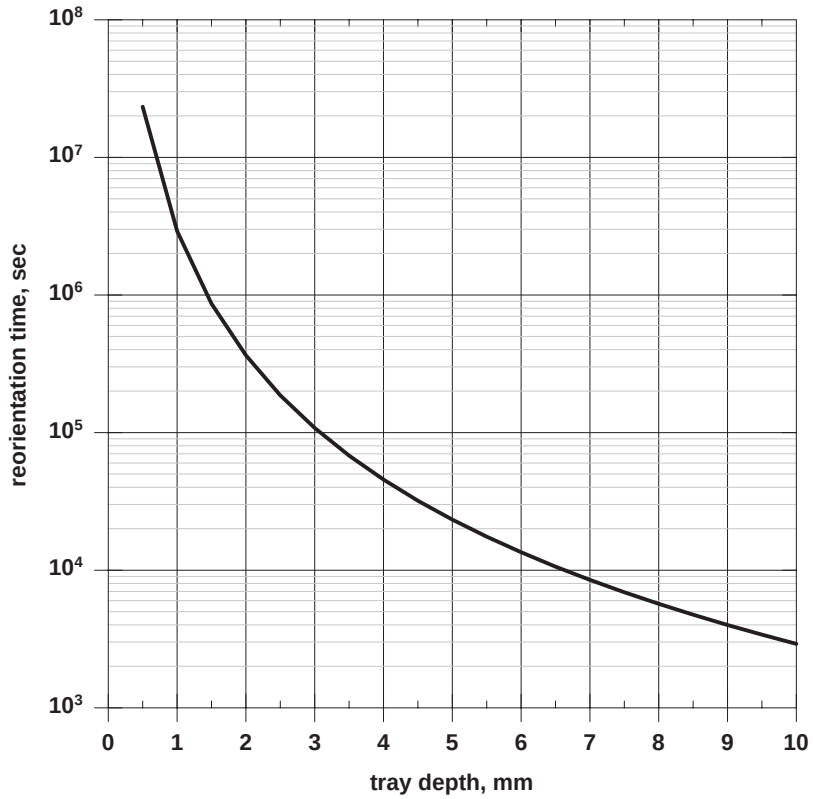

Figure 15. Reorientation time of n-butanol as a function of fuel tray depth. The length of the fuel tray is fixed at 300 mm. For the SAL-5 fuel tray, the reorientation time is 101 hours. These times are only order of magnitude.

REPORT DOCUMENTATION PAGE

Form Approved
OMB No. 0704-0188

1. AGENCY USE ONLY (*Leave blank*)	2. REPORT DATE	3. REPORT TYPE AND DATES COVERED
	September 2004	Final Contractor Report

4. TITLE AND SUBTITLE

Analysis of the Spread Across Liquid–5 (SAL–5) Experiment Failure to Fill Properly During Flight

5. FUNDING NUMBERS

WBS–22–101–58–09
NCC3–975

6. AUTHOR(S)

Jeffrey S. Allen

7. PERFORMING ORGANIZATION NAME(S) AND ADDRESS(ES)

National Center for Microgravity Research
21000 Brookpark Road
Cleveland, Ohio 44135

8. PERFORMING ORGANIZATION REPORT NUMBER

E–14777

9. SPONSORING/MONITORING AGENCY NAME(S) AND ADDRESS(ES)

National Aeronautics and Space Administration
Washington, DC 20546–0001

10. SPONSORING/MONITORING AGENCY REPORT NUMBER

NASA CR—2004-213317

11. SUPPLEMENTARY NOTES

Project Manager, Kathy Schubert, Microgravity Science Division, NASA Glenn Research Center, organization code 6700, 216–433–5331.

12a. DISTRIBUTION/AVAILABILITY STATEMENT

Unclassified - Unlimited
Subject Category: 34 Distribution: Nonstandard

Available electronically at http://gltrs.grc.nasa.gov

This publication is available from the NASA Center for AeroSpace Information, 301–621–0390.

12b. DISTRIBUTION CODE

13. ABSTRACT ***(Maximum 200 words)***

When a pool of flammable liquid is ignited, the flame spread rate can vary widely depending on the initial fuel temperature, pool geometry, ambient atmospheric conditions, and gravitational level. There is substantial decades-old debate in the scientific literature about the role of gravity in these phenomena. The objective of the research was to measure ignition and flame spread across liquid pools in both normal and microgravity with and without forced airflow, and to obtain detailed thermal and velocity field data for comparison to a predictive numerical model that is concurrently being developed. To that end, an experiment known as Spread Across Liquids–5 (SAL–5) was designed to be conducted in a low-gravity environment on a sounding rocket. Unfortunately, during the sounding rocket flight the fuel tray for the experiment failed to fill properly prior to ignition. The primary cause of the failure to fill properly is the geometry of the fuel tray; that is, the presence of the gaps on the side walls and the sharp edge around the thermocouple through-holes. The contamination resulting from the cleaning process is a strong secondary factor which would have prevented proper, timely filling had the primary cause not been present.

14. SUBJECT TERMS

Capillary flow; Spreading; Wetting

15. NUMBER OF PAGES

32

16. PRICE CODE

17. SECURITY CLASSIFICATION OF REPORT	18. SECURITY CLASSIFICATION OF THIS PAGE	19. SECURITY CLASSIFICATION OF ABSTRACT	20. LIMITATION OF ABSTRACT
Unclassified	Unclassified	Unclassified	